On the principles underyling the diagnosis of brain tumors - A survey article

Go, K.G.; Kamman, R.L.; Pruim, J.; Hew, J.M.; Vaalburg, A.M.J.; Mooyart, E.L.; Heesters, M.A.A.M.; Lopes da Silva, F.H.; Paans, W.

DOI
10.1007/BF02307407

Publication date
1995

Published in
Acta neurochirurgica

Acta Neurochir (Wien) (1995) 135: 1–11

Acta Neurochirurgica

On the Principles Underlying the Diagnosis of Brain Tumours – A Survey Article

K. G. Go[1], R. L. Kamman[2], J. Pruim[4], J. M. Hew[3], W. Vaalburg[4], A. M. J. Paans[4], E. L. Mooyaart[2], M. A. A. M. Heesters[5], F. H. Lopes da Silva[6]

Departments of [1]Neurosugery, Diagnostic Radiology, Sections of [2]Magnetic Resonance Imaging and [3]Neuroradiology, [4]Positron Emission Tomography, [5]Radiotherapy, University Hospital Groningen, and [6]Institute of Neurobiology, University of Amsterdam, The Netherlands

Summary

A survey is given of the principles underlying the diagnosis of brain tumours.

Traditionally diagnosis and localization of brain tumours have been based upon morphological criteria. Currently unsurpassed levels in imaging of anatomical details and topographical relations by the techniques of computed tomography (CT) and magnetic resonance imaging (MRI) have been achieved.

The techniques of positron emission tomography (PET) and of magnetic resonance spectroscopy (MRS), which depict also metabolic and blood flow aspects, provide a refinement of our knowledge on the metabolism, structure and pathophysiological relations of a tumour to the surrounding parenchyma.

Recent advances in the recording of function-related changes of the cerebral electro-magnetic field allow a better definition of critical functional areas.

Keywords: Brain tumour; brain oedema; blood brain barrier.

Brain tumours possess several characteristics, many of which have proved useful for their diagnosis (Table 1). As the original meaning of *tumour = swelling* denotes, brain tumours are primarily known by their nature as *space occupying lesions*. This is not surprising as they tend to present themselves clinically with the signs and symptoms of increased intracranial pressure, in view of the rigidity of the cranial box which allows no expansion. The diagnostic techniques then available, such as angiography and pneumo- encephalography or ventriculography, truely represented this space occupying character, responsible for displacements of the blood vessels, and displacement or compression of cerebrospinal fluid (CSF) spaces, although a few tumours could be directly visualised during angiography bei their possession of an abnormal vascular network.

As the current techniques of computerised tomography (CT) and magnetic resonance imaging (MRI) demonstrate, it may not only be the tumour itself that is responsible for this expansive effect, but also the *peritumoural oedema* (*οἴδημα* being the Greek rendering of Latin *tumor* for swelling) which usually sur-

Table 1. *Aspects of Brain Tumours Relevant to Diagnosis*

1. Space-occupying nature

→ Morphology of expansion: displacement of surrounding structures on angiogram, CT, MRI
→ Signs and symptoms of intracranial hypertension (and eventual coning)

2. Blood-brain barrier impairment

→ Vasogenic oedema around tumour on CT and MRI
→ Contrast enhancement on CT and MRI
tracer exudation on isotope scan

3. Metabolic changes

(A) Prevalence of aerobic glycolysis

→ Increased glucose consumption (^{18}FDG PET)
→ Increased lactate production (LAC in ^{1}H-MRS)

(B) Cellular proliferation

→ Increased protein biosynthesis and incorporation of amino acids ^{11}C-TYR & ^{11}C-MET PET
→ Increased membrane biosynthesis (CHOL in ^{1}H-MRS)

4. Local neuronal damage

→ Signs and symptoms of loss of local function
→ Local changes of electrical activity on EEG
local changes of magnetic field on MEG
→ Loss of NAA in ^{1}H-MRS

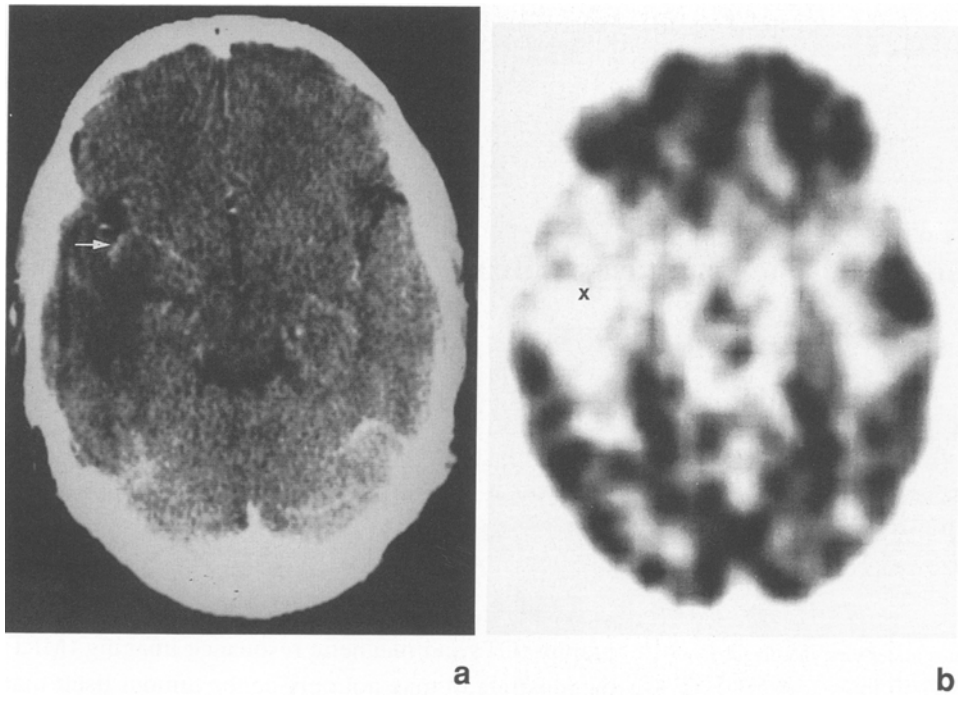

Fig. 1. (a) CT-scan of a patient with a low-grade astrocytoma showing an extensive area of hypodensity in the right temporal pole; there is no enhancement of the tumour in spite of contrast filling the middle cerebral artery (arrow). (b) ^{18}FDG-PET scan of the patient of (a) visualising a corresponding area of reduced FDG uptake (x), suggesting a low-grade glioma, which was subsequently proved by biopsy

rounds the tumour to a greater or lesser extent (Figs. 1a and 3a). Peritumoural brain oedema is regarded as a type of vasogenic brain oedema, which is the consequence of blood-brain barrier impairment and exudation of blood plasma into the brain parenchyma, contrary to cytotoxic brain oedema, which is intracellularly located and occupies both grey and white matter as one may observe in recent infarctions. Vasogenic oedema has the propensity to occupy white matter, and has the appearance of areas of hypodensity on CT or hyperintensity on T2-weighted MRI-scans, with fingerlike extensions in accordance with the shape of the white matter. As to the genesis of peritumoural oedema, it may be considered to bear upon the type of tumour with respect to classification into intra-axial tumours (gliomas), extra-axial tumours (meningiomas and neurinomas), and metastatic tumours. As gliomas arise from the brain tissue itself and tend to infiltrate the surrounding tissue, there is no definite border separating the tumour from the surrounding tissue and restricting the flow of oedema fluid into the surrounding tissue; in the glioma the exudate especially originates in the marginal regions in which the blood-brain barrier is disrupted as shown by contrast studies. But not all gliomas constitute a solid mass of tumour; a histological study of serial stereotaxic biopsies has demonstrated, that low-grade gliomas may consist of isolated neoplastic cells scattered within the brain parenchyma rather than a central mass of tumour (Daumas-Duport *et al.* 1987). Extra-axial tumours arise outside the brain; from the cerebral white matter in which oedema fluid tends to accumulate, these tumours are separated by several layers being the arachnoid mater, the subarachnoid space, the pia mater, and the cerebral cortex, all of

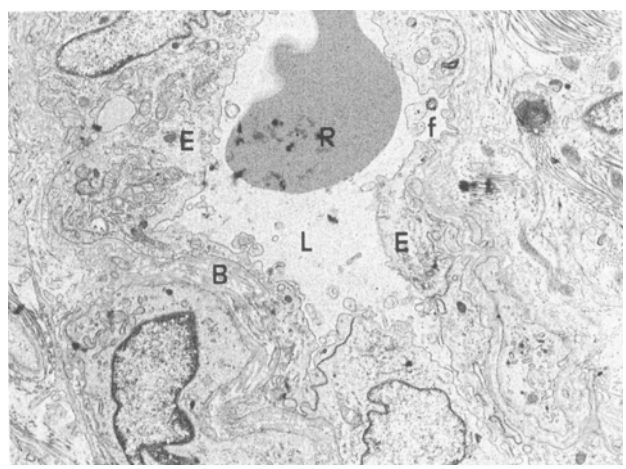

Fig. 2. Electron micrograph of capillary wall in a malignant astrocytoma, showing fenestration (*f*). *L* capillary lumen; *R* red blood cell; *E* endothelial cell; *B* basement membrane

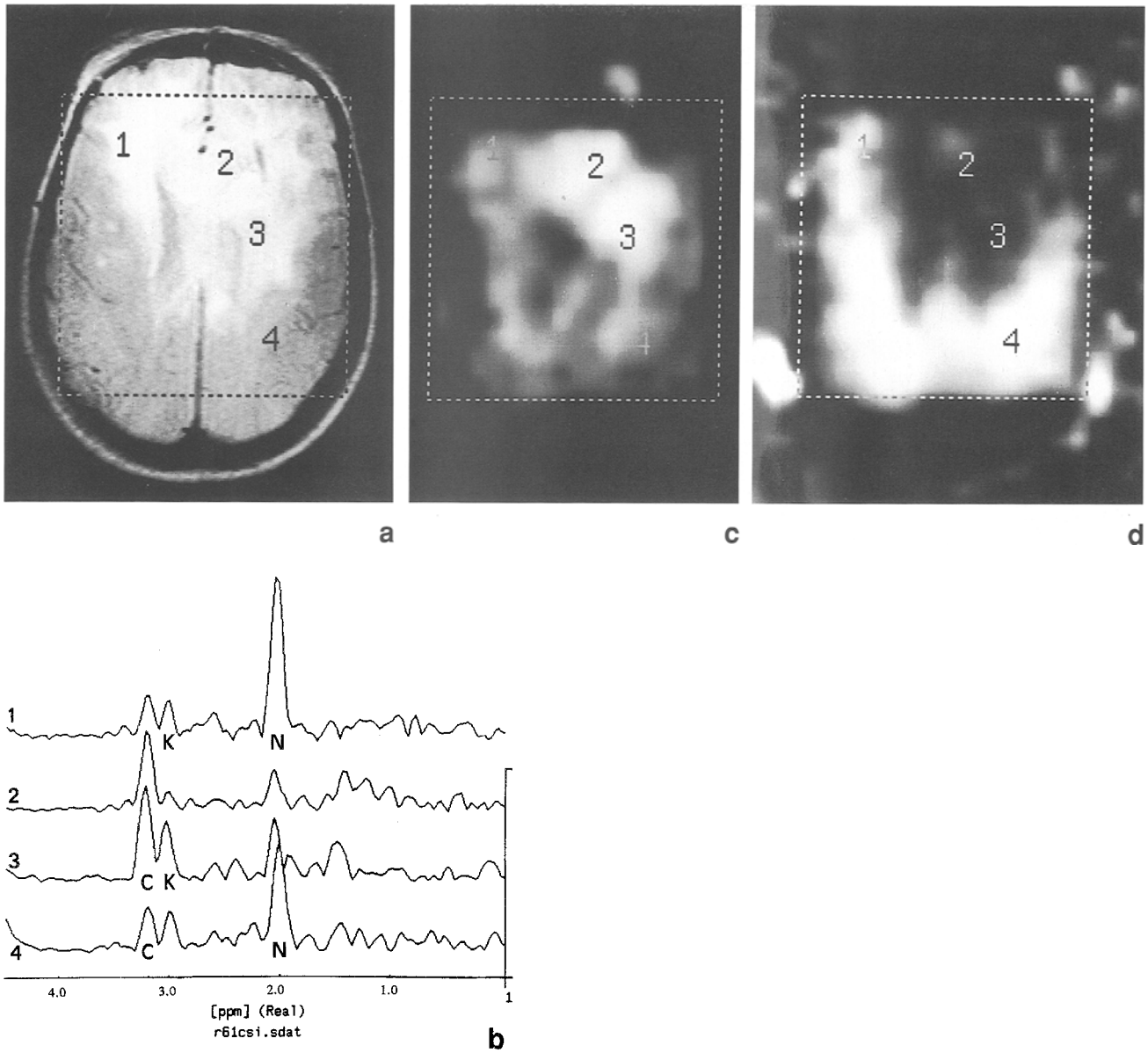

Fig. 3. (a) T_2-weighted MRI of a frontal oligodendroglioma with extensive peritumoural oedema. The box denotes the area, for which the proton MR spectroscopic images of choline and NAA (c, d) are available. The numbers denote the regions, of which the MR spectra are shown in (b). (b) Proton MR-spectra from the areas, denoted by the numbers on the MRI (a). The abscissa shows the chemical shifts of the resonance frequency, characterising the metabolites: choline (*C*) at 3.2, creatine (*K*) at 3.0, NAA (*N*) at 2.0 ppm (parts per million), lactate is not visible here. The right frontal area (*1*), which showed oedema on the MRI (a), does not seem to contain any tumour, since there are normal choline and NAA peaks; the left frontal area (*2*) and left median area (*3*) are probably the sites of the tumour, with elevated choline peaks, and decreased NAA peaks; while the left occipital area (*4*) again shows normal choline and NAA peaks. Compare with (a), in which the real site of the tumour is obscured by the extensive oedema. (c) Proton MRSI, choline map of the patient of (a), showing the distribution of choline in the area marked by the box. The high choline contents at the site of the tumour (*2* and *3*) are clearly visible, compared to the areas (*1* and *4*) not containing tumour. (d) Proton MRSI, NAA map of the same patient of (a), visualising the distribution of the neurone-marker NAA in the area within the box. The location of the tumour (*2* and *3*) is conspicuous by the absence of NAA, denoting replacement of the neuronal population by neoplastic cells. Note that the oedematous area *1* does contain NAA

which tend to impede to some degree the spread of oedema fluid from the tumour. As has been demonstrated, in meningiomas the amount of peritumoural oedema appeared to depend not only on the size and histological type of the tumour, but also on the integrity of the separating layers, and to correlate with the exudation of contrast agent (Go *et al.* 1988; 1993). Although metastases are usually well demarcated

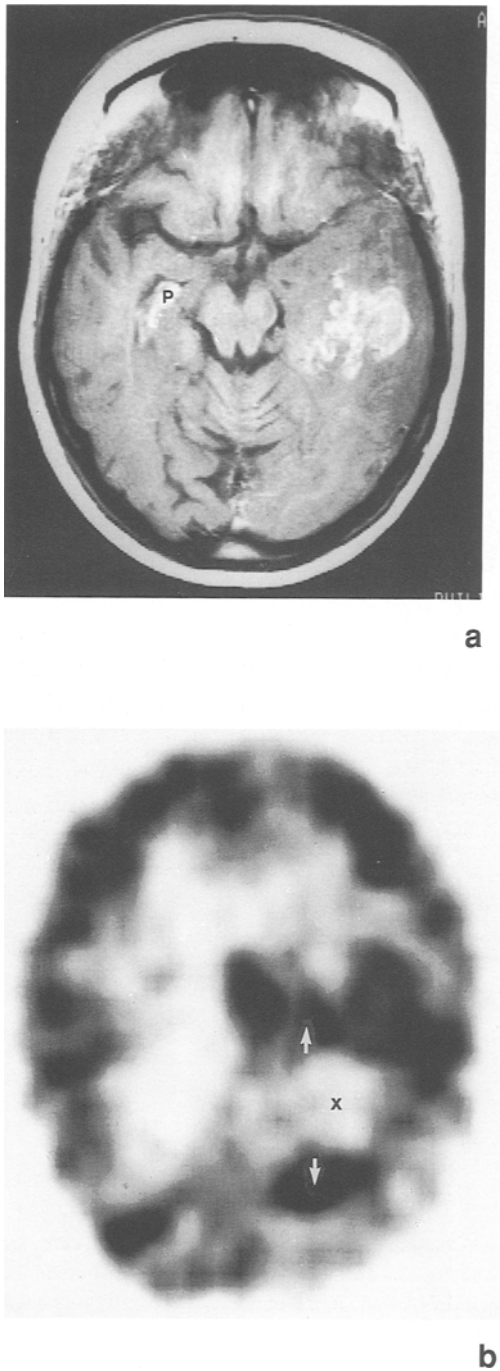

Fig. 4. (a) Tl-weighted Gd-enhanced MRI of a patient in whom 6 years before a left temporo-occipital oligodendroglioma had been resected and irradiated, and now exhibited new complaints and a right-sided hemianopia. In the left median temporal region there was now a garlandlike structure of contrast enhancement suggestive of recurrence or radionecrosis. *P* choroid plexus of the right temporal horn, being a circumventricular organ devoid of a blood-brain barrier, and therefore showing contrast enhancement. (b) ^{18}FDG-PET scan of the patient of (a), showing a highly reduced FDG uptake at the original location of the tumour (*x*), consistent with radionecrosis; but elevated FDG uptake in frontal and occipital areas (arrows), denoting recurrent tumours

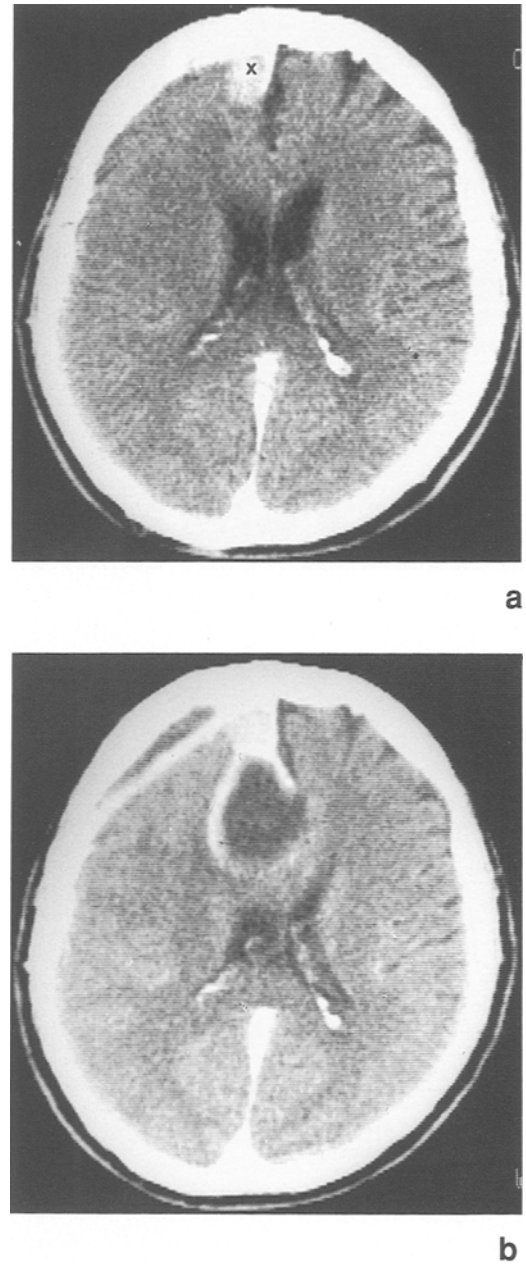

Fig. 5. (a) Contrast-enhanced CT-scan made 3 days after resection of a tumour (an astrocytoma according to pre-operative histology) in the right frontal pole; there was extensive contrast exudation in the walls of the cavity, initially suggesting extensive residual tumour, but in fact due to operative blood-brain barrier damage. (b) Contrast-enhanced CT-scan made 6 months later showed the real extent of the residual tumour (*x*), which in the meantime proved to be a meningioma

from surrounding brain, they are intra-axially located and not enveloped by layers which may impede the spread of oedema fluid from the tumour into the surrounding brain. With meningiomas and metastases,

the oedema fluid also originates from the tumour, since contrast studies demonstrate that the blood-brain barrier is not disrupted in the surrounding brain.

Underlying causes of the *disruption of the blood-brain barrier in tumours* are abnormalities of the endothelium in the capillaries of the tumour (Hirano and Matsui 1975, Long 1970). These especially include fenestrations, and abnormalities of the junctions between the endothelial cells (Fig. 2). Fenestrations are thin areas of the endothelial cytoplasm, through which blood-borne substances may pass into the brain parenchyma. In the normal brain fenestrated capillary endothelium is found only in the circumventricular organs such as the pineal gland, the choroid plexus, and a few other structures around the ventricles, which possess no blood-brain barrier (Fig. 4a). In the early days, when angiography and ventriculography were used to detect brain tumours, these rather behaved like phantoms which were not directly visible, but only betrayed themselves by the displacement of surrounding blood vessels or ventricles. Brain isotope scanning (scintigraphy) was the only method capable of directly visualising a tumour by the uptake of radioactive tracer entering the tumour on account of a deficient blood-brain barrier. In the modern era of CT- and MRI-scanning, diagnosis on the basis of blood-brain barrier impairment still constitutes a valuable principle, as enhancement of the tumour following intravenous administration of contrast agents may demarcate a tumour from surrounding oedema. Early enhancement, however, with contrast agent still contained within the blood vessels, may rather represent the extent of microvascularisation of the tumour (Daumas-Duport *et al.* 1987). The pattern of enhancement, although not pathognomonic, may point to the type of tumour: homogeneous enhancement is seen in extra-axial tumours such as meningiomas and neurinomas, heterogeneous enhancement exhibiting garland-like patterns occur with glioblastomas, in which rims of enhancement are also seen, as in some oligodendrogliomas and metastases; while fine streaks of enhancement tend to occur in astrocytomas.

Apart from enhancement, a tumour may possess *density characteristics on CT or specific T_1 and T_2 values on MRI,* which may differentiate it from normal brain without the employment of contrast agent. Thus the majority of gliomas appear hypodense on CT (Fig. 1 a), except medulloblastomas and ependymomas, which tend to be slightly hyperdense; also meningiomas and lymphomas tend to be hyperdense. With conventional T_2W MRI (Figs. 3 a and 6 b), most astrocytomas appear isointense to grey matter, as do

Table 2. *Cellular Metabolism in Tissue Proliferation*

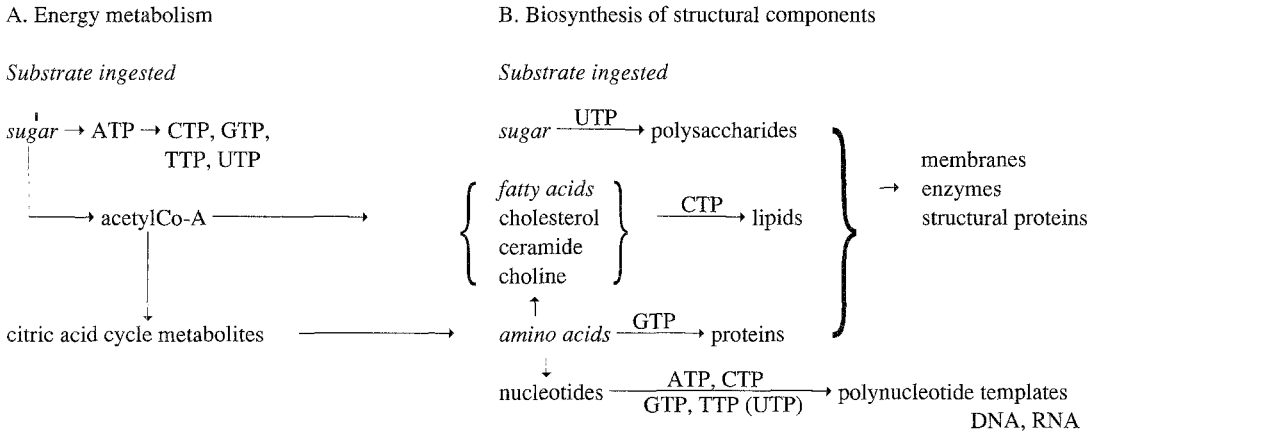

Energy metabolism which particularly comprises the oxidation of sugar, subserves the production of adenosine triphosphate (*ATP*), the cellular currency driving several energy consuming cellular reactions. ATP also serves to obtain other nucleoside triphosphates, such as uridine triphosphate (*UTP*), which drives the biosynthesis of polysaccharides, cytosine triphosphate (*CTP*), driving the biosynthesis of lipids, and guanosine triphosphate (*GTP*) driving the biosynthesis of proteins. Among the various substrates in food, sugar provides the building blocks for polysaccharides, but its metabolism in glycolysis is also the source of acetylcoenzyme A, which serves as the precursor of amino acids, and lipid constituents, such as ceramide and cholesterol. Choline, another lipid constituent, derives from the amino acid methionine. The amino acids also provide the nucleotides, from which the polynucleotide templates (*DNA* and *RNA*) for the biosynthesis of proteins, are synthesised using the various nucleotide triphosphates as energy sources. The polysaccharides, lipids, and proteins constitute enzymes, structural proteins and membranes, which form the structural components of the newly formed cells in tissue proliferation.

oligodendrogliomas, whereas meningiomas tend to be more hypo-intense to grey matter. Obviously, these features possess too little specificity to warrant a specific identification of the type of tumour in the individual case.

But even CT- and MRI-scanning only depict brain tumours by their *morphologic* aspects, be it directly on account of their special features, be it by deficiency of the blood-brain barrier or by their familiar property of displacing surrounding structures. In fact the mere signs of a space occupying lesion are *non-specific* and may not be sufficient to diagnose a tumour, as infarctions, cystic lesions, inflammatory lesions (abscesses), or radionecrosis may present with the same signs of expansion. Similarly, blood-brain barrier breakdown, causing enhancement by contrast agents must be regarded as a non-specific feature (Fig. 4 a). A reason for confusion is for example, the blood- brain barrier disruption shortly after a surgical resection, causing extensive enhancement of the wound cavity and posing as residual tumour (Fig. 5 a and b).

The recent techniques of *positron emission tomography (PET) and proton magnetic resonance spectroscopy (MRS)* have allowed the diagnosis of brain tumours on account of their *metabolic* features. It pertains to the effects, which the presence of tumours may have on cerebral metabolism. The space occupying character of the tumour and of accompanying oedema may raise intracranial pressure, initially in the vicinity of the tumour, compromising regional tissue perfusion, but eventually in a global way, causing more widespread ischaemia. On the other hand, metabolites produced by the tumour may cause hyperaemia and increase of local tissue blood flow. A reduction of blood flow has been observed by means of ^{99m}Tc-HMPAO single photon emission computed tomography (SPECT) in many low-grade and in some high-grade gliomas, while other malignant gliomas exhibited increased blood flow (Maier-Hauff *et al.* 1990). The possibility of ischaemia has been substantiated by measurements of tissue oxygen tension, which demonstrated low values in tumours and in the area of peritumoural oedema (Kayama *et al.* 1991). Apart from these blood flow-related changes of energy metabolism, tumours in general may exhibit a prevalence of (aerobic) glycolysis for their provision of energy (Warburg 1956). Moreover, tumours tend to show changes of metabolism which are intimately related to their neoplastic nature, pertaining to the biosynthesis of cellular constituents such as proteins and membranes (Table 2).

Using positron-emitting tracers of physiological metabolic substrates, PET allows the study of substrate uptake. Substrates are taken up by the brain for consumption in energy metabolism, or for incorporation into cellular constituents. A study on the uptake of ^{18}F-deoxy-D-glucose (^{18}FDG) demonstrated elevated glucose consumption in high-grade gliomas, which is probably related to the predominance of glycolysis. The increase of ^{18}FDG-uptake appeared to be correlated to short survival times in patients (Patronas *et al.* 1985). Apart from the other instance of elevated glucose consumption, i.e., in epileptic foci during seizures, an increase of ^{18}FDG-uptake in a lesion may therefore be considered to indicate its neoplastic nature. Elevated ^{18}FDG-uptake (Fig. 4 b) has been employed to differentiate recurrence of tumour from radionecrosis in cases which could not be resolved by the conventional imaging techniques (Doyle *et al.* 1987). However, not all gliomas exhibit an increase of ^{18}FDG-uptake; the low-grade gliomas in particular, may show a reduced ^{18}FDG-uptake with respect to normal brain (Fig. 1 b). Decrease of ^{18}FDG-uptake, on the other hand, is a less specific finding, since infarctions, epileptic foci in the interictal period, and other lesions involving loss of tissue, all display a reduced ^{18}FDG-uptake. Absence of ^{18}FDG-uptake appearing as a metabolic void may point to necrosis or a cystic lesion (Go *et al.* 1993).

The demonstration by PET of an increased uptake of amino acid tracers in the lesion with respect to normal brain, such as that of [^{11}C-methyl]-L-methionine (^{11}C-MET), also indicates a neoplastic nature of the lesion, in which the amino acid is presumably being accumulated in the process of increased protein biosynthesis by the proliferating tissue (Ogawa *et al.* 1993). As a measure of protein biosynthesis, however, methyl-labelled methionine seems to be less appropriate, as methionine tends to be the main biochemical source of methylgroups (Ishiwata *et al.* 1988). To evaluate the rate of protein biosynthesis therefore carboxylic-labelled amino acids, such as L-[1-^{11}C] tyrosine (^{11}C-TYR), have a greater potential, if both the metabolic profile and the quantity of metabolites are known (Paans *et al.* 1993), although the radiochemical synthesis for PET is less easy to perform (Fig. 6a). ^{11}C-TYR uptake may be used to localise cerebral gliomas for stereotaxic biopsy or resection in instances, in which the tumour is deep-seated

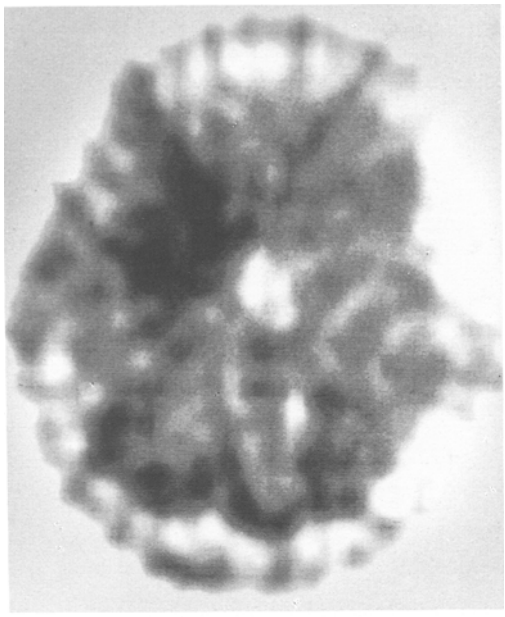

a

b

Fig. 6. (a) ^{11}C-TYR PET-scan of patient with glioma visualising increased ^{11}C-TYR uptake in the right frontal area. (b) For comparison, T_2-weighted MRI of the same patient of (a), depicting hyperintensity in the corresponding right frontal area

or located at a critial site with respect to function, while absence of contrast enhancement on CT- and MR-scans makes a precise location uncertain (Go *et al.* 1994).

Apart from the investigation of metabolism, PET allows the assessment of blood-brain barrier integrity by means of ^{68}Ga-EDTA, which has been undertaken in a study on brain tumours in conjunction with ^{11}C-MET (Bergström *et al.* 1983). Using $^{15}O_2$ and $H_2{}^{15}O$ as tracers, PET has been employed to measure oxygen consumption and blood flow, respectively, in brain tumours. Thus a reduction of oxygen consumption could be demonstrated in brain tumours after radiochemotherapy (Ogawa *et al.* 1988).

A technique which uses a conventional 1.5 Tesla MR-apparatus but requires appropriate adaptations (such as special coils) and soft-ware implementation is proton magnetic resonance spectroscopy (^{1}H-MRS), especially of proton containing metabolites that occur in adequate concentration in tissue, such as phosphocholine (CHOL), (phospho)creatine (CREAT), N-acetylaspartate (NAA), and lactate (LAC) (Go 1991). These metabolites appear as resonance peaks of marked height in the proton magnetic resonance spectrum (Fig. 3 b). The substance (or a specific proton containing group it contains) is characterised by its place on the abscissa of the spectrum, which denotes the specific chemical shift of resonance frequency it exhibits on the basis of the specific molecular environment of the proton delivering the signal. Signals of adequate size may be obtained from a volume of tissue of 1 ml. Consequently unit volumes of tissue (voxels) of 1 cm^3 may be chosen to make up the total volume of brain to be studied, an in magnetic resonance spectroscopic imaging (MRSI) reconstructed into two-dimensional matrices representing the spatial distribution of a certain metabolite in the total volume studied (Fig. 3c and d). CHOL appears to be abundant in gliomas as a constituent of membrane components to be incorporated in the growing cells of the tumour. CREAT occurs in all living cells, subserving energy metabolism as creatine phosphate, and is often used as a reference to express the relative concentrations of the other metabolites. NAA is a component of neurones, the function of which is still poorly understood. Its disappearance in tumours presumably indicates that the normal neuronal population in the lesion has been replaced by tumour cells. With respect to functionally critical areas it may be important to establish whether disappearance of the NAA signal in such an area in the lesion warrants resection of the area without risking further deterioration of function. LAC also tends to be elevated in tumours, presumably on the basis of the predominance of glycolysis, although another cause may be impaired perfusion due to elevated regional tissue pressure. On the

basis of the elevation of CHOL, and decrease of NAA, MRSI appears to be useful in localising low-grade gliomas for stereotaxic biopsy, in cases in which this was not feasible by the current imaging techniques, and which would have resulted in negative biopsies. The elevation of CHOL in gliomas tends to occur in the marginal rather than in the central parts of the tumour. In patients in whom MRSI and PET have been conducted, the pattern of CHOL elevation seemed to resemble that of ^{11}C-TYR uptake; indeed it is cellular proliferation that underlies both findings. Other instances of CHOL elevation, although with a different distribution, may be found in multiple sclerosis, in which demyelination is associated with remyelination. LAC elevation occurs with the high-grade gliomas, in particular, and tends to be located in the core of the tumour rather than in its margin, possibly suggesting necrosis. Among other structural details which can be recognised is the occurrence of associated cysts which contain high levels of LAC (Go *et al.* 1993). LAC elevation per se is nonspecific, as it conceivably occurs in infarction. Similarly, loss of the NAA signal only denotes loss of the neuronal population, and may occur in infarctions as well. Following radiotherapy there is decrease of the elevated CHOL and LAC signals in some tumours, but no recovery of the lost NAA signal (Heesters *et al.* 1993). Recurrence of tumour has been differentiated from radionecrosis on the basis of the CHOL signal (Ott *et al.* 1993).

Magnetic resonance spectroscopy of tissue phosphorus compounds (^{31}P-MRS) has demonstrated changes in brain tumours, such as a reduction of creatine phosphate suggesting involvement of energy metabolism, and decreases of phosphomono- and phosphodiesters, which presumably pertain to changes of phosphocholine metabolism related to membrane biosynthesis. Measurement of tissue pH on the basis of the pH-induced shift of the inorganic phosphate peak indicated an alkaline rather than an acid environment (Hubesch *et al.* 1990). Unfortunately, the low concentration of phosphorus compounds in tissue makes the technique rather insensitive, requiring about 100 ml of tissue to provide an adequate signal.

Apart from its behaviour as a space-occupying lesion, brain tumours may cause local *impairment of function*, the signs and symptoms of which conceivably depend on the location of the tumour and the specific function residing at the location. In this respect it

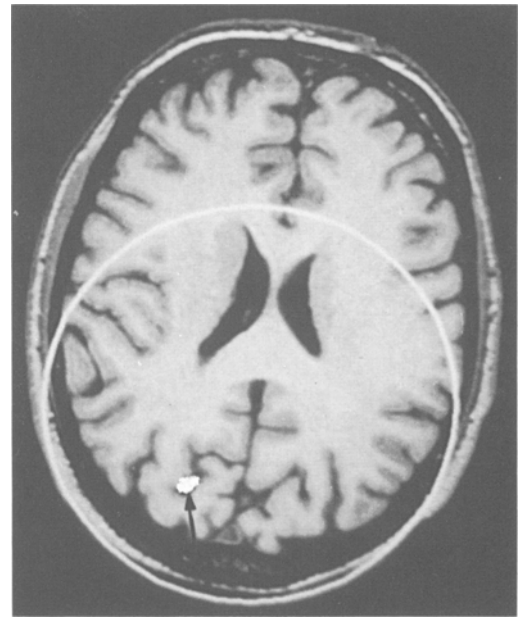

Fig. 7. Presentation on MRI of an active equivalent dipole source (white field at arrow point), obtained from magneto-encephalogram recorded at several locations, during selective visual attention directed to the contralateral side

is interesting, that clinical analysis of brain tumours associated with peritumoural oedema has revealed that loss of neurological function rather correlated with the site of the tumour, such as paresis of the left leg with a metastasis in the leg area of the right motor cortex, than with the oedema, which on the CT-scans occupied a larger area of the cerebral hemisphere, involving the motor areas of the left arm and face as well. Moreover, in the oedematous areas the sensory evoked responses showed reaction times which were similar to those in the controlateral hemisphere (Penn 1980).

The *impairment of neurological* function may be considered to result from the disturbance of neuronal function, and this may have its repercussions on *electrical activity*, as it becomes manifest in the *electroencephalogram*. Notably, the EEG changes observed with tumours are slow waves in the overlying areas. Clinical as well as experimental evidence has demonstrated that for the genesis of these polymorphic delta waves the interruption of important afferent inputs to the cerebral cortex is responsible, caused by lesions in the white matter, or in the thalamus, the hypothalamus, and the brainstem (Gloor *et al.* 1977). In addition to EEG, magneto-encephalography (MEG) may record the changes of the magnetic field associated

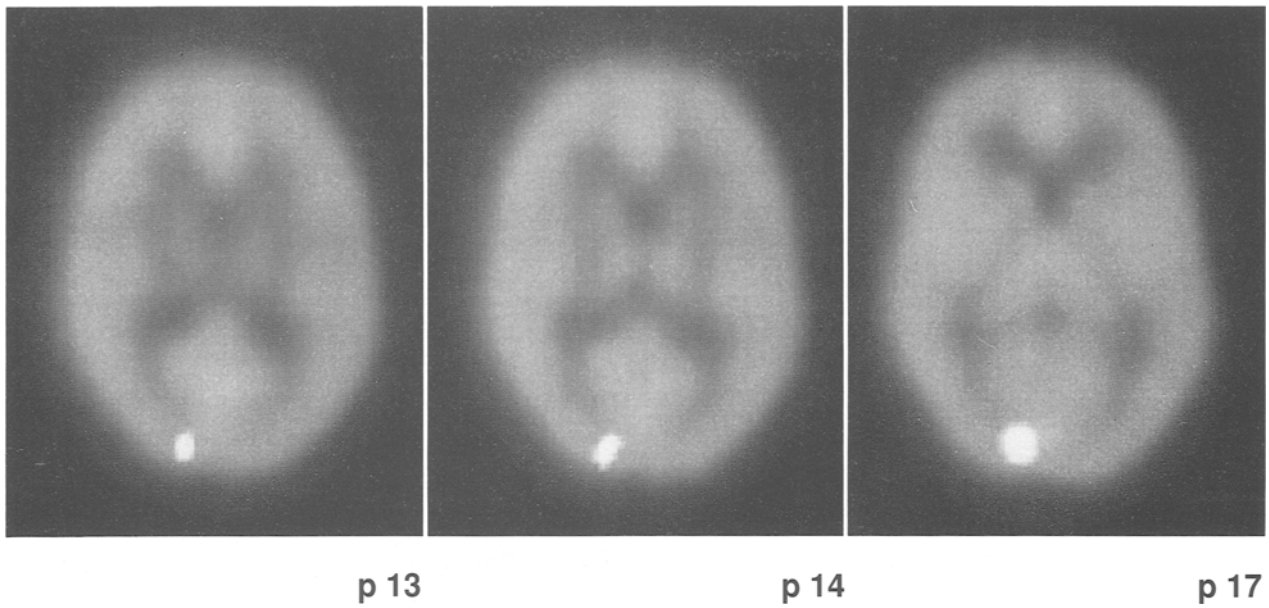

Fig. 8. Multiple slice PET-scan of volunteer with $H_2{}^{15}O$ as a tracer to visualise cerebral blood flow, showing activation with increase of blood flow in the left occipital visual field, during visual field stimulation

with those of the electrical field. By means of mathematical models, the source of the electrical activity in the EEG, or that of the magnetic field changes on the MEG, may be identified as a so-called equivalent dipole, and allows the localisation of important functional areas, such as those subserving vision, speech or motor function (Fig. 7) (Lopes da Silva *et al.* 1991; Wieringa *et al.* 1993). Localisation of functional areas has traditionally been achieved on the basis of blood flow measurement by the ^{133}Xe inhalation technique, or by PET using $H_2{}^{15}O$ as a tracer (Fig. 8) (Go 1991). It may also be attained by means of functional MR-imaging, by which changes of blood oxygenation and of blood flow that are induced in cortical areas by the performance of motor, visual or mental tasks, may be visualised in the MR image (Kwong *et al.* 1992). Future prospects of diagnosis in brain tumours therefore include a combination of conventional MR imaging with MR-angiography and functional MR-imaging or PET to visualise relevant vascular structures and critical functional areas which are to be avoided during the intervention. The images may be reconstructed 3-dimensionally, which facilitates spatial insight, and is conceivably important in topographically complex regions (viz. the pineal and suprasellar regions). Visualisation of the brain surface with its cortical topography (Kalada 1990), allowing the superposition of functional and metabolic data, obtained by PET or MRS (Kapoulcas *et al.* 1991) may be significant in the recognition of functionally critical cortical areas. Moreover, the equivalent dipole source obtained by EEG or MEG data may also be superimposed on a three-dimensional reconstruction of the brain.

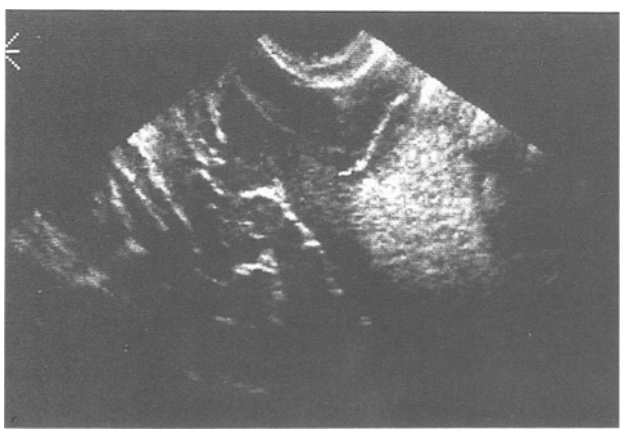

Fig. 9. Intra-operative ultrasound depicting a subcortical glioma in the parietal motor area

In the *intra-operative* situation, as early as 1923 Grant has applied the measurement of electrical tissue impedance to detect a tumour. It is based upon the decrease of the resistance of the tissue to low-frequency alternative electric current, caused by the presence of extracellular oedema around the tumour

(Go *et al.* 1973). Another technique which has been applied to visualise tumours during operation constituted the intravenous injection of fluorescein dye, which crosses the disrupted blood-brain barrier and stains the tumour (Moore 1950). A recent valuable contribution to the localisation of deeply seated tumours during operation is the use of ultrasound (Fig. 9), which can visualise surrounding oedema and associated cysts; the echogenicity of the lesion is determined by the presence of interfaces between tissue structures with different acoustic densities, which therefore can reflect ultrasound (Chandler and Knake 1984).

References

1. Bergström M, Collins VP, Ehrin E, Ericson K, Eriksson L, Greitz T, Halldin C, Von Holst H, Langstrom B, Lilja A, Lundqvist H, Nagren K (1983) Discrepancies in brain tumor extent as shown by computed tomography and positron emission tomography using [68Ga]EDTA, [11C]glucose, and [11C]methionine. J Comp Ass Tomogr 7: 1062–1066
2. Chandler WF, Knake JE (1984) Intraoperative use of ultrasound in neurosurgery. Clin Neurosurg 31: 550–563
3. Daumas-Duport C, Monsaigneon V, Blond S, Munari C, Musolino A, Chodkiewicz JP, Missir O (1987) Serial stereotactic biopsies and CT scan in gliomas: correlative study in 100 astrocytomas, oligo-astrocytomas and oligodendrogliomas. J Neurooncol 4: 317–328
4. Doyle WK, Budinger TF, Valk PE, Levin VA, Gutin PH (1987) Differentiation of cerebral radiation necrosis from tumor recurrence by [18F]FDG and 82Rb positron emission tomography. Neurosurgery 11: 563–570
5. Gloor P, Ball G, Schaul N (1977) Brain lesions that produce delta waves in the EEG. Neurology 27: 326–333
6. Go KG, Hew JM, Kamman RL, Molenaar WM, Pruim J, Blaauw EH (1993) Cystic lesions of the brain. A classification based on pathogenesis, with consideration of histological and radiological features. Eur J Radiol 17: 69–84
7. Go KG, Van der Veen PH, Ebels EJ, Van Woudenberg F (1972) A study of electrical impedance of oedematous cerebral tissue during operations. Acta Neurochir (Wien): 113–124
8. Go KG (1991) Cerebral pathophysiology. An integral approach with some emphasis on clinical implications. Elsevier, Amsterdam
9. Go KG, Wilmink JT, Molenaar WM (1988) Peritumoral brain edema associated with meningiomas. Neurosurgery 23: 175–179
10. Go KG, Keuter EJW, Kamman RL, Pruim J, Metzemaekers JDM, Staal MJ, Paans AMJ, Vaalburg W (1994) The contribution of magnetic resonance spectroscopic imaging and L-[1-^{11}C]-tyrosine positron emission tomography to localization of cerebral gliomas for biopsy. Neurosurgery 34: 994–1002
11. Go KG, Kamman RL, Wilmink JT, Mooyaart EL (1993) A study on peritumoural brain oedema around meningiomas by CT and MRI scanning. Acta Neurochir (Wien): 41–46
12. Grant FC (1923) Localization of brain tumors by determination of the electrical resistance of the growth. JAMA 81: 2169–2171
13. Heesters MAAM, Kamman RL, Mooyaart EL, Go KG (1993) Localized proton spectroscopy of inoperable brain gliomas. Response to radiation therapy. J Neurooncol 17: 27–35
14. Hirano A, Matsui T (1975) Vascular structures in brain tumors. Human Pathol 6: 611–621
15. Hubesch B, Sappey-Marinier D, Roth K, Meyerhoff DJ, Matson GB, Weiner MW (1990) P31 MR spectroscopy of normal human brain and brain tumors. Radiology 174: 401–409
16. Ishiwata K, Vaalburg W, Elsinga PH, Paans AMJ, Woldring MG (1988) Comparison of L-[1-11C]methionine and L-methyl-[11C]methionine for measuring in vivo protein synthesis rates with PET. J Nucl Med 29: 1419–1427
17. Kapouleas I, Alavi A, Alves WM, Gur RE, Weiss DW (1991) Registration of three-dimensional MR images of the human brain without markers. Radiology 181: 731–739
18. Katada K (1990) MR imaging of brain surface structures; surface anatomy scanning (SAS). Neuroradiology 32: 439–448
19. Kwong KK, Belliveau JW, Chesler DA, Goldberg IE, Weisskoff RM, Poncelet BP, Kennedy DN, Hoppel BE, Cohen MS, Turner R, Cheng HM, Brady TJ, Rosen BR (1992) Dynamic magnetic resonance imaging of human brain activity during primary sensory stimulation. Proc Natl Acad Sci USA 89: 5675–5679
20. Long DM (1970) Capillary ultrastructure and the blood-brain barrier in human malignant brain tumors. J Neurosurg 32: 127–144
21. Lopes da Silva FH, Spekreijse H (1991) Localization of brain sources of visually evoked responses: using single and multiple dipoles. An overview of different approaches. Eventrelated Brain Research [EEG Suppl] 42: 38–46
22. Maier-Hauff K, Gerlach L, Cordes M (1990) HM-PAO-SPECT in the differentiation of cerebral gliomas. First experiences with blood flow measurements. In: Schneider GH, Vogler E, Kocever K (eds) Digitale Bildgebung, interventionelle Radiologie, integrierte digitale Radiologie. Blackwell Ueberreuter, pp 40–46
23. Moore GE (1950) Diagnosis and localization of brain tumors. Thomas, Springfield
24. Ogawa T, Uemura K, Shishido F, Yamaguchi T, Murakami M, Inugami A, Kanno I, Sasaki H, Kato T, Hirata K, Kowada M, Mineura K, Yasuda T (1988) Changes of cerebral blood flow, and oxygen and glucose metabolism following radiochemotherapy of gliomas. A PET study. J Comp Ass Tomogr 12: 290–297
25. Ogawa T, Shishido F, Kanno I, Inugami A, Fujita H, Murakami M, Shimosegawa E, Ito H, Hatazawa J, Okudera T, Uemura K, Yasui N, Mineura K (1993) Cerebral glioma: evaluation with methionine PET. Radiology 186: 45–53
26. Ott D, Hennig J, Ernst T (1993) Human brain tumors: assessment with in vivo proton MR spectroscopy. Radiology 186: 745–752
27. Paans AMJ, Elsinga PH, Vaalburg W (1993) Carbon-11 labeled tyrosine as a probe for modelling the protein synthesis rate. In: Mazoyer BM, Heiss WD, Comar D (eds) PET studies on amino acid metabolism and protein synthesis. Kluver, Boston, pp 161–174
28. Patronas NJ, Di Chiro G, Kufta C, Bairamian D, Kornblith PL, Simon R, Larson SM (1985) Prediction of survival in glioma

patients by means of positron emission tomography. J Neurosurg 62: 816–822
29. Penn RD (1980) Cerebral edema and neurological function CT, evoked responses and clinical examination. Adv Neurol 28: 383–394
30. Warburg O (1956) On the origin of cancer cells. Science 123: 309–314
31. Wieringa HJ, Peters MJ, Lopes da Silva FH (1993) The estimation of a realistic localization of dipole layers within the brain based on functional (EEG, MEG) and structural (MRI) data: a preliminary note. Brain Topogr 5: 327–330

Correspondence: K. G. Go, M.D., Department of Neurosurgery, Academisch Ziekenhuis Groningen, Oostersingel 59, Postbus 30.001, NL-9700 RB Groningen, The Netherlands.